Science
AAAS

Title: Long-term changes in moisture, not CO_2, are the primary driver of woody cover change in the tropics

Authors: William D. Gosling[1]*, Charlotte S. Miller[2], Timothy M. Shanahan[3], Philip B. Holden[4], Jonathan T. Overpeck[5], and Frank van Langevelde[6,7]

Affiliations:

[1] Institute for Biodiversity & Ecosystem Dynamics, University of Amsterdam, The Netherlands.

[2] Leeds Trinity University, Leeds, United Kingdom.

[3] Department of Geological Sciences, University of Texas at Austin, United States of America.

[4] School of Environment, Earth & Ecosystem Sciences, The Open University, United Kingdom.

[5] School for Environment & Sustainability, University of Michigan, United States of America.

[6] Department of Environmental Sciences, Wageningen University & Research, The Netherlands.

[7] School of Life Sciences, University of KwaZulu-Natal, South Africa.

Abstract: Anthropogenically elevated CO_2 (eCO_2) levels have been suggested to increase woody cover within tropical ecosystems through fertilization. The effect of eCO_2 is built into Earth system models, although testing the relationship over long periods of time remains challenging. Here we explore the relative importance of six drivers of vegetation change in western Africa over the last *c.* 500,000 years (moisture availability, fire activity, mammalian herbivore density, temperature, temperature seasonality, CO_2) by coupling past environmental change data from Lake Bosumtwi (Ghana) with global data. We find that moisture availability and fire activity were the most important factors in determining woody cover, whereas the effect of CO_2 was small. Our findings suggest that the role of eCO_2 effects on tropical vegetation in predictive models must be reconsidered.

One Sentence Summary: CO_2 does not dominate woody vegetation dynamics in the tropics.

Main Text:

Tropical vegetation forms an important part of the global carbon cycle, with forests contributing 33% *(1)* and savannas 30% *(2)* of the global terrestrial net primary productivity. The current paradigm suggests that anthropogenically elevated CO_2 (eCO_2) levels have enhanced carbon sequestration rates in tropical forests *(3, 4)* and resulted in elevated woody cover, 'greening', within tropical savannas and grasslands *(5-7)*. The suggested reason for these changes is that plant species that use the C_3 photosynthetic pathway (such as trees and shrubs) are predicted to sequester more carbon under eCO_2 than species that use the C_4 pathway (such as tropical grasses) *(8, 9)*. This highly influential concept of tropical 'greening' due to eCO_2 is difficult to test, especially on large spatial scales or over long periods of time *(10-12)*. However, dynamic global vegetation and Earth system models, which are used to predict the impacts of projected future climate change, nevertheless typically include a fertilization effect of eCO_2 on the growth of woody cover in the tropics, *e.g., (6, 13-16)*.

The impact of eCO_2 on vegetation has recently been challenged in observational and experimental field studies running over decades *(17-20)*; with atmospheric CO_2 rising by c. 100 ppm since AD 1960 (NOAA Global Monitoring Lab). Consequently, a significant question now exists regarding the effect of eCO_2 on vegetation community change (*e.g.*, shift in the dominance of plants with C_3 *versus* C_4 photosynthetic pathways), rather than on individual plants, and therefore on the importance of including eCO_2 as driver of vegetation change in models over long periods of time and on large spatial scales. This is fundamental to understanding Earth system function because it took thousands of years for modern tropical forest vegetation to establish following the end of the last global glacial period, *e.g., (21)*. Furthermore, if we are to be able to correctly anticipate future vegetation change, and predict the potentially significant roles that vegetation could play in mitigating, or enhancing, climate change under continuing anthropogenic eCO_2 levels, it is over long periods of time that knowledge is required. While modelling studies have been used to assess how lower eCO_2 levels could have impacted vegetation during the latter part of the last glacial period, *c.* 21-18,000 years ago *(22-24)*, there remains, currently, no data available to support the causal relationship between eCO_2 and tropical woody cover over multiple high magnitude (>100 ppm) eCO_2 transitions relevant to the establishment of tropical vegetation communities. Here we remedy this problem and explore the relationship between tropical woody cover, CO_2, and five other variables known to influence woody cover (fire activity, mammalian herbivore density, moisture availability, temperature, and temperature seasonality *(25-27)*) over the last *c.* 500,000 years at a site in tropical western Africa.

The sedimentary archive recovered from Lake Bosumtwi in Ghana (6°30'N, 1°25'W, 97 m above sea level) contains evidence for multiple multi-millennial transitions between tropical woody and grass-dominated vegetation over the last *c.* 500,000 years *(28, 29)*. Located within moist semi-evergreen forest today, Bosumtwi receives *c*. 1450 mm of rainfall per year *(30)*. To the north of Bosumtwi there is a concomitant decline in rainfall and woody cover *(31)*. The relationship between the depth and age of the sediments recovered from Bosumtwi is constrained independently by radiocarbon, optically stimulated luminescence and uranium-thorium ages. All these data are combined through a Bayesian probability model to allow uncertainties in the chronology to be calculated (Fig. 1S; *(32)*). The exceptionally long record of past environmental changes, and its position on ecological and climatic gradients, makes Bosumtwi the ideal location to test the relative importance of drivers of tropical vegetation dynamics *(21)*. Furthermore, the variation in woody cover in the Bosumtwi record and the simulated vegetation carbon storage show similar, sub-100,000 year, patterns of change over the last c. 500,000 years *(33)* (Fig. 1A, B).

We characterize the woody cover in tropical western Africa, and the likely factors driving change, using a combination of observed and simulated data obtained from the sedimentary core recovered from Bosumtwi *(34)*, the GENIE-1 Earth system (climate-carbon cycle) model *(35)*, and ice core records *(36)*. Four variables were obtained from Bosumtwi (pollen taxa, charcoal fragments, *Sporormiella* fungal spores, and $\delta^{15}N$) providing time series of vegetation cover (variation of woody *versus* grassy cover), fire activity, mammalian herbivore density, and moisture availability respectively *(32)*. Two additional variables were obtained for the Bosumtwi region from the GENIE-1 model, namely temperature and temperature seasonality *(33)*. Atmospheric CO_2 concentrations were taken from ice-core records *(36)*. The data sets were integrated using an updated chronology for Bosumtwi *(32)*, the chronology from within the GENIE-1 model *(35)*, and the ice core chronology *(36)*.

The data extracted from the Bosumtwi sediment core show variations in the degree of woody cover (Fig. 1B), fire activity (Fig. 1C), mammalian herbivore density (Fig. 1D), and moisture availability (Fig. 1E). The major variation in the pollen assemblage over the last *c.* 500,000 years is driven primarily by the abundance of grass (Poaceae) (Fig. 1B *(28, 29, 32)*). Fire activity and mammalian herbivores are shown to have been near continually present in the landscape for the last *c.* 500,000 years; with the lowest prevalence of fire activity being after *c.* 9000 years ago, and the lowest density of mammalian herbivores between *c.* 22,000 and 800 years ago. Moisture availability is shown to oscillate throughout the last *c.* 500,000 years with lower-than-average availability suggested between *c.* 300,000 and 130,000, and around 30,000 years ago (Fig. 1E). Temperature (Fig. 1F), temperature seasonality (Fig. 1G) and atmospheric CO_2 levels (Fig. 1H) show major fluctuations on 100,000-year and 21,000-year time scales, related to orbital climate forcing *(33)*.

The direction and strength of the relationships between the various variables were assessed through structural equation modelling (SEM, e.g., *(25)*). SEM identifies the directionality of linear relationships within an *a priori* model of seven variables (Fig. 2A *(32)*), calculated independently over two different intervals of time (*c.* 150,000-0 years and 500,000-0 years). The *c.* 150,000-year interval was selected because this section of the sedimentary archive contains the largest number of independent radiometric age control points, *i.e.,* the chronological control is the most robust through this section of the record. The *c.* 500,000-year interval was used because it includes the largest amount of available data on past ecological and climatic change (pollen, *Sporormiella* fungal spores and charcoal fragments with n=112; $\delta^{15}N$ with n=51). The SEM was constructed to examine hypothesized direct and indirect relationships based on current understanding of tropical vegetation *(25, 31)* (Fig. 2A). To explore for possible bias due to chronological uncertainty in the Bosumtwi record the SEMs were also run against 1000 possible alternative versions of the chronology *(28)* for both intervals of time (for the *c.* 500,000-year data see Fig. 3; other analysis in *(32)*). Given the limitations of null-hypothesis significance testing *(37)*, we focused on the relative importance of the predictor variables using the distribution of the standardized coefficients of the SEMs.

Regardless of time interval, moisture availability is shown to be the most important driver of woody cover, directly and indirectly, on multi-millennial time (Fig. 2B, C; Fig. 3; Table S1). Increasing moisture availability simultaneously results in increasing woody cover and a decrease in grass-fuelled fire activity. This decrease likely reflects changes in the abundance of the woody component of these ecosystems, resulting in the negative relationships between fire activity and woody cover *(38)*. Mammalian herbivore density shows a strong positive relationship with fire activity and woody cover. These findings are in agreement with recent analyses indicating that herbivore biomass and woody cover are positively correlated when woody cover is sparse *(26)*. Conversely, increasing temperature seasonality had a strong negative effect on woody cover. These findings are in line with those based on recent global observational studies in savannas *(25, 27, 31)* and forests *(39)*, and additionally suggests that the mechanistic controls on tropical woody cover have remained stable for at least the last half a million years. Surprisingly, the effect of atmospheric CO_2 on woody cover both directly and indirectly, via temperature, was small during the last *c.* 500,000 years at Bosumtwi (Fig. 2B, C); furthermore, even when temperature or moisture were excluded from the SEM the relative importance of the different drivers was found to hold (presented in *(32)*).

Our findings suggest that abiotic (moisture availability and fire activity) and biotic (mammalian herbivore density) drivers operating at the landscape scale together with temperature seasonailty can override the role of CO_2 in driving woody growth at forest-savanna transitions in the tropics. The absence of strong relationship between CO_2 and woody cover at Bosumtwi provides new evidence against the idea that lower eCO_2 levels could be mainly responsible for tropical vegetation change over glacial-interglacial cycles *(22)*, and supports findings of a stronger role for precipitation than CO_2 in determining the position of the treeline in African mountain regions *(23, 24)*. Comparison of major vegetation shifts identified in other long terrestrial records from Africa reveals no strong and contrasting correlation with each other and shifts in global CO_2 (Fig. S7 and S8; *(32)*). In eastern Africa during the last *c.* 500,000 years the periods of highest woody cover (lowest abundance of grasses) at Lake Magadi and Lake Malawi are antiphased *(40-42)* suggesting that a regionally specific change (such as in precipitation pattern *sensu (43)*), rather than a uniform CO_2 fertilisation effect, is likely to be the driving factor. Shorter records from southern (Vankervelsvlei *(44)*) and central (Lake Bambili *(45)*) Africa show changes in woody cover during the last glacial cycle (last *c.* 100,000 years) that do not all occur in concert with global CO_2 shifts, again suggesting other processes were important. A recent analysis of African climate change over the last 1 million years revealed that the major change in precipitation patterns occurred *c.* 300,000 years ago and was related to a shift in tropical climate systems (Walker Circulation) *(43, 46)*. Based on the strong control of moisture availability on woody cover shown here we hypothesise that changes in moisture availability are likely to exerted a greater control on vegetation across Africa than CO_2.

The low relative importance of CO_2 to determining woody cover in Africa over long timescales can be considered mechanistically. Although trees require more carbon to deploy a unit of leaf area than grasses *(5)*, and they need to allocate large amounts of carbon in roots to re-sprout after grass fire and herbivory damage *(47, 48)*, as well as to ensure that they rapidly attain sizes needed to prevent these damages *(49)*, eCO2 may not necessarily result in higher woody cover. Possible explanations for the small CO_2 effect on woody cover are that it can be counteracted by impacts from climate-driven changes *(50)*, by water or nutrient limitations on vegetation productivity *(17)*, or fire could limit woody cover expansion in tropical grasslands and savannas *(21)*, but see *(27)*. Generating comparable, and high resolution, multi-proxy records to test our findings in different biomes across the tropics is now a priority.

Our study confirms that an improved understanding of vegetation community change (C_4 *versus* C_3 plant response) under eCO_2 is needed for dynamic global vegetation and Earth system modelling of the future. The small effects of CO_2 on past woody cover challenges the long-term capacity of tropical savannas and forests to slow anthropogenically eCO_2 through increased 'greening' as woody taxa recruitment and growth are enhanced through CO_2 fertilisation effects, as predicted by these models *(14-16)*. Consequently, our findings suggest that the long-term effectiveness of proposed tropical vegetation-based strategies to mitigate anthropogenic eCO_2 through enhanced carbon sequestration rates *(51, 52)* is contingent on sufficient moisture availability.

References and Notes:

1. R. A. Houghton, Aboveground forest biomass and the global carbon balance. *Global Change Biol.* **11**, 945-958 (2005).

2. J. Grace, J. S. José, P. Meir, H. S. Miranda, R. A. Montes, Productivity and carbon fluxes of tropical savannas. *J. Biogeogr.* **33**, 387-400 (2006).
3. O. L. Phillips *et al.*, Changes in the carbon balance of tropical forests: Evidence from long-term plots. *Science.* **282**, 439-443 (1998).
4. S. L. Lewis, J. Lloyd, S. Sitch, E. T. Mitchard, W. F. Laurance, Changing ecology of tropical forests: Evidence and drivers. *Annual Review of Ecology, Evolution, and Systematics.* **40**, 529-549 (2009).
5. W. J. Bond, G. F. Midgley, A proposed CO2-controlled mechanism of woody plant invasion in grasslands and savannas. *Global Change Biol.* **6**, 865-869 (2000).
6. S. I. Higgins, S. Scheiter, Atmospheric CO2 forces abrupt vegetation shifts locally, but not globally. *Nature.* **488**, 209 (2012).
7. Z. Zhu *et al.*, Greening of the Earth and its drivers. *Nature Climate Change.* **6**, 791-795 (2016).
8. E. A. Ainsworth, S. P. Long, What have we learned from 15 years of free-air CO_2 enrichment (FACE)? A meta-analytic review of the responses of photosynthesis, canopy properties and plant production to rising CO_2. *New Phytol.* **165**, 351-372 (2005).
9. J. R. Ehleringer, T. E. Cerling, B. R. Helliker, C_4 photosynthesis, atmospheric CO_2, and climate. *Oecologia.* **112**, 285-299 (1997).
10. D. D. Breshears *et al.*, Regional vegetation die-off in response to global-change-type drought. *Proc. Natl. Acad. Sci. U. S. A.* **102**, 15144-15148 (2005).
11. H. D. Adams *et al.*, Temperature sensitivity of drought-induced tree mortality portends increased regional die-off under global-change-type drought. *Proc. Natl. Acad. Sci.* **106**, 7063-7066 (2009).
12. R. J. Norby, D. R. Zak, Ecological lessons from free-air CO_2 enrichment (FACE) experiments. *Annual Review of Ecology, Evolution, and Systematics.* **42**(2011).
13. S. P. Harrison, C. I. Prentice, Climate and CO_2 controls on global vegetation distribution at the last glacial maximum: Analysis based on palaeovegetation data, biome modelling and palaeoclimate simulations. *Global Change Biol.* **9**, 983-1004 (2003).
14. S. Sitch *et al.*, Evaluation of the terrestrial carbon cycle, future plant geography and climate-carbon cycle feedbacks using five Dynamic Global Vegetation Models (DGVMs). *Global Change Biol.* **14**, 2015-2039 (2008).
15. P. M. Cox *et al.*, Sensitivity of tropical carbon to climate change constrained by carbon dioxide variability. *Nature.* **494**, 341-344 (2013).
16. C. Huntingford *et al.*, Simulated resilience of tropical rainforests to CO_2-induced climate change. *Nature Geoscience.* **6**, 268-273 (2013).
17. S. Wang *et al.*, Recent global decline of CO2 fertilization effects on vegetation photosynthesis. *Science.* **370**, 1295-1300 (2020).
18. P. Groenendijk *et al.*, No evidence for consistent long-term growth stimulation of 13 tropical tree species: Results from tree-ring analysis. *Global Change Biol.* **21**, 3762-3776 (2015).
19. P. van der Sleen *et al.*, No growth stimulation of tropical trees by 150 years of CO_2 fertilization but water-use efficiency increased. *Nat. Geosci.* **8**, 24-28 (2015).
20. P. B. Reich, S. E. Hobbie, T. D. Lee, M. A. Pastore, Unexpected reversal of C_3 versus C_4 grass response to elevated CO_2 during a 20-year field experiment. *Science.* **360**, 317-320 (2018).
21. T. M. Shanahan *et al.*, CO_2 and fire influence tropical ecosystem stability in response to climate change. *Scientific Reports.* **6**, 29587 (2016).
22. D. Jolly, A. Haxeltine, Effect of low glacial atmospheric CO_2 on tropical African montane vegetation. *Science.* **276**, 786-788 (1997).
23. H. Wu, J. Guiot, S. Brewer, Z. Guo, Climatic changes in Eurasia and Africa at the last glacial maximum and mid-Holocene: Reconstruction from pollen data using inverse vegetation modelling. *Climate Dynamics.* **29**, 211-229 (2007).
24. K. Izumi, A. Lézine, Pollen-based biome reconstructions over the past 18,000 years and atmospheric CO2 impacts on vegetation in equatorial mountains of Africa. *Quaternary Science Reviews.* **152**, 93-103 (2016).
25. C. E. R. Lehmann *et al.*, Savanna vegetation-fire-climate relationships differ among continents. *Science.* **343**, 548-552 (2014).
26. G. P. Hampson, S. Archibald, W. J. Bond, A continent-wide assessment of the form and intensity of large mammal herbivory in Africa. *Science.* **350**, 1056-1061 (2015).
27. E. M. Veenendaal *et al.*, On the relationship between fire regime and vegetation structure in the tropics. *New Phytol.* **218**, 153-166 (2018).

28. C. S. Miller, W. D. Gosling, Quaternary forest associations in lowland tropical West Africa. *Quaternary Science Reviews*. **84**, 7-25 (2014).
29. C. S. Miller, W. D. Gosling, D. B. Kemp, A. L. Coe, I. Gilmour, Drivers of ecosystem and climate change in tropical West Africa over the past ~540 000 years. *Journal of Quaternary Science.* **31**, 671-677 (2016).
30. T. M. Shanahan, J. T. Overpeck, W. E. Sharp, C. A. Scholz, J. A. Arko, Simulating the response of a closed-basin lake to recent climate changes in tropical West Africa (Lake Bosumtwi, Ghana). *Hydrological Processes.* **21**, 1678-1691 (2007).
31. M. Sankaran *et al.*, Determinants of woody cover in African savannas. *Nature.* **438**, 846-849 (2005).
32. See online Supplementary Materials.
33. W. D. Gosling, P. B. Holden, Precessional forcing of tropical vegetation carbon storage. *Journal of Quaternary Science.* **26**, 463-467 (2011).
34. C. Koeberl *et al.*, The ICDP Lake Bosumtwi drilling project: A first report. *Scientific Drilling.* **1**, 23-27 (2005).
35. P. B. Holden *et al.*, Interhemispheric coupling, the West Antarctic ice sheet and warm Antarctic interglacials. *Climate of the Past.* **6**, 431-443 (2010).
36. D. Lüthi *et al.*, High-resolution carbon dioxide concentration record 650,000–800,000 years before present. *Nature.* **453**, 379-382 (2008).
37. D. R. Anderson, K. P. Burnham, W. L. Thompson, Null hypothesis testing: Problems, prevalence, and an alternative. *The Journal of Wildlife Management.* **64**, 912-923 (2000).
38. F. van Langevelde *et al.*, Effects of fire and herbivory on the stability of savanna ecosystems. *Ecology.* **84**, 337-350 (2003).
39. O. L. Phillips *et al.*, Drought sensitivity of the Amazon rainforest. *Science.* **323**, 1344-1347 (2009).
40. V. M. Muiruri *et al.*, A million year vegetation history and palaeoenvironmental record from the Lake Magadi Basin, Kenya Rift Valley. *Palaeogeography, Palaeoclimatology, Palaeoecology.* **567**, 110247 (2021).
41. R. B. Owen *et al.*, Progressive aridification in East Africa over the last half million years and implications for human evolution. *Proc. Natl. Acad. Sci.* **115**, 11174-11179 (2018).
42. S. J. Ivory, A. Lézine, A. Vincens, A. S. Cohen, Waxing and waning of forests: Late Quaternary biogeography of southeast Africa. *Global Change Biol.* **24**, 2939-2951 (2018).
43. S. Kaboth-Bahr *et al.*, Paleo-ENSO influence on African environments and early modern humans. *Proc. Natl. Acad. Sci.* **118**, e2018277118 (2021).
44. L. J. Quick *et al.*, Vegetation and climate dynamics during the last glacial period in the fynbos-afrotemperate forest ecotone, southern Cape, South Africa. *Quaternary International.* **404**, 136-149 (2016).
45. A. Lézine, K. Izumi, M. Kageyama, G. Achoundong, A 90,000-year record of Afromontane forest responses to climate change. *Science.* **363**, 177-181 (2019).
46. W. D. Gosling, E. M. L. Scerri, S. Kaboth-Bahr, The climate and vegetation backdrop to hominin evolution in Africa. *Philosophical Transactions of the Royal Society B: Biological Sciences.* **377**, 20200483 (2022).
47. K. W. Tomlinson *et al.*, Biomass partitioning and root morphology of savanna trees across a water gradient. *J. Ecol.* **100**, 1113-1121 (2012).
48. C. C. Boonman *et al.*, On the importance of root traits in seedlings of tropical tree species. *New Phytol.* **227**, 156-167 (2020).
49. A. M. Hoffman, J. A. Bushey, T. W. Ocheltree, M. D. Smith, Genetic and functional variation across regional and local scales is associated with climate in a foundational prairie grass. *New Phytol.* (2020).
50. J. Liu *et al.*, Contrasting carbon cycle responses of the tropical continents to the 2015-2016 El Niño. *Science.* **358**, eaam5690 (2017).
51. M. J. Sullivan *et al.*, Long-term thermal sensitivity of Earth's tropical forests. *Science.* **368**, 869-874 (2020).
52. J. Bastin *et al.*, The global tree restoration potential. *Science.* **365**, 76-79 (2019).
53. T. M. Shanahan *et al.*, Age models for long lacustrine sediment records using multiple dating approaches - An example from Lake Bosumtwi, Ghana. *Quaternary Geochronology.* **15**, 47-60 (2013).
54. C. Koeberl, W. Reimold, J. Blum, C. P. Chamberlain, Petrology and geochemistry of target rocks from the Bosumtwi impact structure, Ghana, and comparison with Ivory Coast tektites. *Geochimica et Cosmochimica Acta.* **62**, 2179-2196 (1998).
55. C. Koeberl *et al.*, An international and multidisciplinary drilling project into a young complex impact structure: The 2004 ICDP Bosumtwi Crater Drilling Project - An overview. *Meteoritics and Planetary Science.* **42**, 483-511 (2007).
56. M. Blaauw, J. A. Christen, Flexible paleoclimate age-depth models using an autoregressive gamma process. *Bayesian Analysis.* **6**, 457-474 (2011).

57. M. Blaauw, Methods and code for 'classical' age-modelling of radiocarbon sequences. *Quaternary Geochronology.* **5**, 512-518 (2010).
58. P. E. Jardine *et al.*, Pollen and spores as biological recorders of past ultraviolet irradiance. *Scientific Reports.* **6**, 39269 (2016).
59. P. E. Jardine *et al.*, Sporopollenin chemistry and its durability in the geological record: an integration of extant and fossil chemical data across the seed plants. *Palaeontology.* **64**, 285-305 (2021).
60. W. D. Gosling *et al.*, Data from: Long-term changes in moisture, not CO2, are the primary driver of woody cover change in the tropics. *FigShare.* (2022). DOI: 10.6084/m9.figshare.18319466
61. P. D. Moore, J. A. Webb, M. E. Collinson, *Pollen Analysis* (Blackwell Scientific, Oxford, ed. 2nd, 1991).
62. J. Stockmarr, Tablets with spores used in absolute pollen analysis. *Pollen Et Spore.* **XIII**, 615-621 (1971).
63. L. von Post, Forest tree pollen in south Swedish peat bog deposits. *Pollen Et Spore.* **9**, 375-401 (English translation by M.B. Davis and K. Faegri from original 1916 lecture; Introduction by K. Faegri and J. Iversen) (1967).
64. H. Godwin, *The History of the British Flora: A Factual Basis for Phytogeography* (Cambridge University Press, Cambridge, 1956).
65. J. G. L. Jacobson, R. H. W. Bradshaw, The selection of sites for paleovegetational studies. *Quaternary Research.* **16**, 80-96 (1981).
66. M. R. Talbot, T. Johannessen, A high resolution palaeoclimatic record for the last 27 500 years in tropical West Africa from the carbon and nitrogen isotopic composition of lacustrine organic matter. *Earth & Planetary Science Letters.* **110**, 23-37 (1992).
67. A. C. M. Julier *et al.*, The modern pollen-vegetation relationships of a tropical forest-savannah mosaic landscape, Ghana, West Africa. *Palynology.* **42**, 324-338 (2018).
68. W. D. Gosling, C. S. Miller, D. A. Livingstone, Atlas of the tropical West African pollen flora. *Review of Palaeobotany and Palynology.* **199**, 1-135 (2013).
69. R. Bonnefille, Atlas des pollens d'Ethiopie. *Adansonia.* **11**, 463-518 (1971).
70. R. Bonnefille, G. Riollet, *Pollens des savanes d'Afrique orientale* (CNRS, Paris, 1980), pp. 140.
71. J. R. Marlon *et al.*, Global biomass burning: A synthesis and review of Holocene paleofire records and their controls. *Quaternary Science Reviews.* **65**, 5-25 (2013).
72. C. Whitlock, C. Larsen, in Tracking Environmental Change Using Lake Sediments Volume 3: Terrestrial, Algal and Siliceous Indicators, J. P. Smol, H. J. B. Birks, W. M. Last, Eds. (Kluwer Academic Publishers, Dordrecht/Boston/London, 2001), pp. 75-98.
73. O. K. Davis, D. S. Shafer, Sporormiella fungal spores, a palynological means of detecting herbivore density. *Palaeogeogr., Palaeoclimatol., Palaeoecol.* **237**, 40-50 (2006).
74. A. G. Baker, P. Cornelissen, S. A. Bhagwat, F. W. M. Vera, K. J. Willis, Quantification of population sizes of large herbivores and their long-term functional role in ecosystems using dung fungal spores. *Methods in Ecology and Evolution.* **7**, 1273-1281 (2016).
75. B. van Geel, A. Aptroot, Fossil ascomycetes in Quaternary deposits. *Nova Hedwigia.* **82**, 313-329 (2006).
76. J. L. Gill, J. W. Williams, S. T. Jackson, K. B. Lininger, G. S. Robinson, Pleistocene megafaunal collapse, novel plant communities, and enhanced fire regimes in North America. *Science.* **326**, 1100-1103 (2009).
77. D. Raper, M. Bush, A test of Sporormiella representation as a predictor of megaherbivore presence and abundance. *Quaternary Research.* **71**, 490-496 (2009).
78. W. D. Gosling *et al.*, Preliminary evidence for green, brown and black worlds in tropical western Africa during the Middle and Late Pleistocene. *Palaeoecology of Africa.* **35**, 13-25 (2021).
79. M. R. Talbot, in Tracking Environmental Change Using Lake Sediments. Volume 2. Physical and Geochemical methods, W. M. Last, J. P. Smol, Eds. (Kluwer Academic Press, Dordrecht/Boston/London, 2001), pp. 401-439.
80. T. B. Coplen, Guidelines and recommended terms for expression of stable-isotope-ratio and gas-ratio measurement results. *Rapid Communications in Mass Spectrometry.* **25**, 2538-2560 (2011).
81. N. R. Edwards, R. Marsh, Uncertainties due to transport-parameter sensitivity in an efficient 3-D ocean-climate model. *Clim. Dyn.* **24**, 415-433 (2005).
82. M. S. Williamson, T. M. Lenton, J. G. Shepherd, N. R. Edwards, An efficient numerical terrestrial scheme (ENTS) for Earth system modelling. *Ecological Modelling.* **198**, 362-374 (2006).
83. D. Lüthi *et al.*, High-resolution carbon dioxide concentration record 650,000–800,000 years before present. *Nature.* **453**, 379-382 (2008).
84. A. Berger, Long-term variations of daily insolation and Quaternary climatic change. *Journal of Atmospheric Science.* **35**, 2362-2367 (1978).
85. W. R. Peltier, Ice age paleotopography. *Science.* **265**, 195-201 (1994).

86. L. E. Lisiecki, M. E. Raymo, A Pliocene-Pleistocene stack of 57 globally distributed benthic d18O records. *Paleoceanography.* **20**, PA1003 (2005).
87. P. B. Holden, N. R. Edwards, K. I. C. Oliver, T. M. Lenton, R. D. Wilkinson, A probabilistic calibration of climate sensitivity and terrestrial carbon change in GENIE-1. *Clim. Dyn.* **35**, 785-806 (2010).
88. B. H. Pugesek, A. Tomer, A. von Eye, Eds., *Structural Equation Modelling: Applications in Ecological and Evolutionary Biology* (Cambridge University Press, Cambridge, 2003).
89. M. Austin, On non-linear species response models in ordination. *Vegetatio.* **33**, 33-41 (1976).
90. Y. Rosseel, lavaan: An R Package for Structural Equation Modeling. *Journal of Statistical Software.* **48**(2012).
91. L. J. Quick *et al.*, Neotoma Dataset 46707: Vankervelsvlei. (2016).
92. A.-M. Lézine, L. Février, K. Lemonnier, Neotoma Dataset 40945: Bambili 2. (2019).
93. P. G. Palmer, S. Gerbeth-Jones, A scanning electron microscope survey of the epidermis of East African grasses, V, and West African supplement. *Smithsonian Contributions to Botany.* **67**, 1-157 (1988).

Acknowledgments: We thank four anonymous reviewers and the editor (Dr. Andrew Sugden) for their extensive comments which have no doubt help improve the quality of this manuscript.

Funding: This past environmental change data from Lake Bosumtwi used in this study was funded by the NERC/The Open University Charter studentship (NE/H525054/1, CSM) and NERC New Investigator Award (NE/G000824/1, WDG). We thank the Lake Bosumtwi Drilling Project team, the International Continental Drilling Program, and the U.S. National Science Foundation for supporting the acquisition of Bosumtwi sediment cores and age model data.
Author contributions: The manuscript was conceived and developed by WDG and FvL. The past environmental change data from Bosumtwi was generated by CSM and WDG. The statistical analysis was conducted by FvL. Expertise on past climate change and the Bosumwti sedimentary record was provided by TMS and JTO. Expertise on Earth system modeling was provided by PBH. The manuscript was written by WDG and FvL, with contributions from all authors. **Competing interests:** The authors declare no conflicts of interest. **Data and materials availability:** The past environmental change data reported in this manuscript is archived in Figshare: DOI: 10.6084/m9.figshare.18319466

Supplementary Materials:

Materials and Methods

Supplementary Text

Figure S1-S8

Tables S1

References (*52-93*)

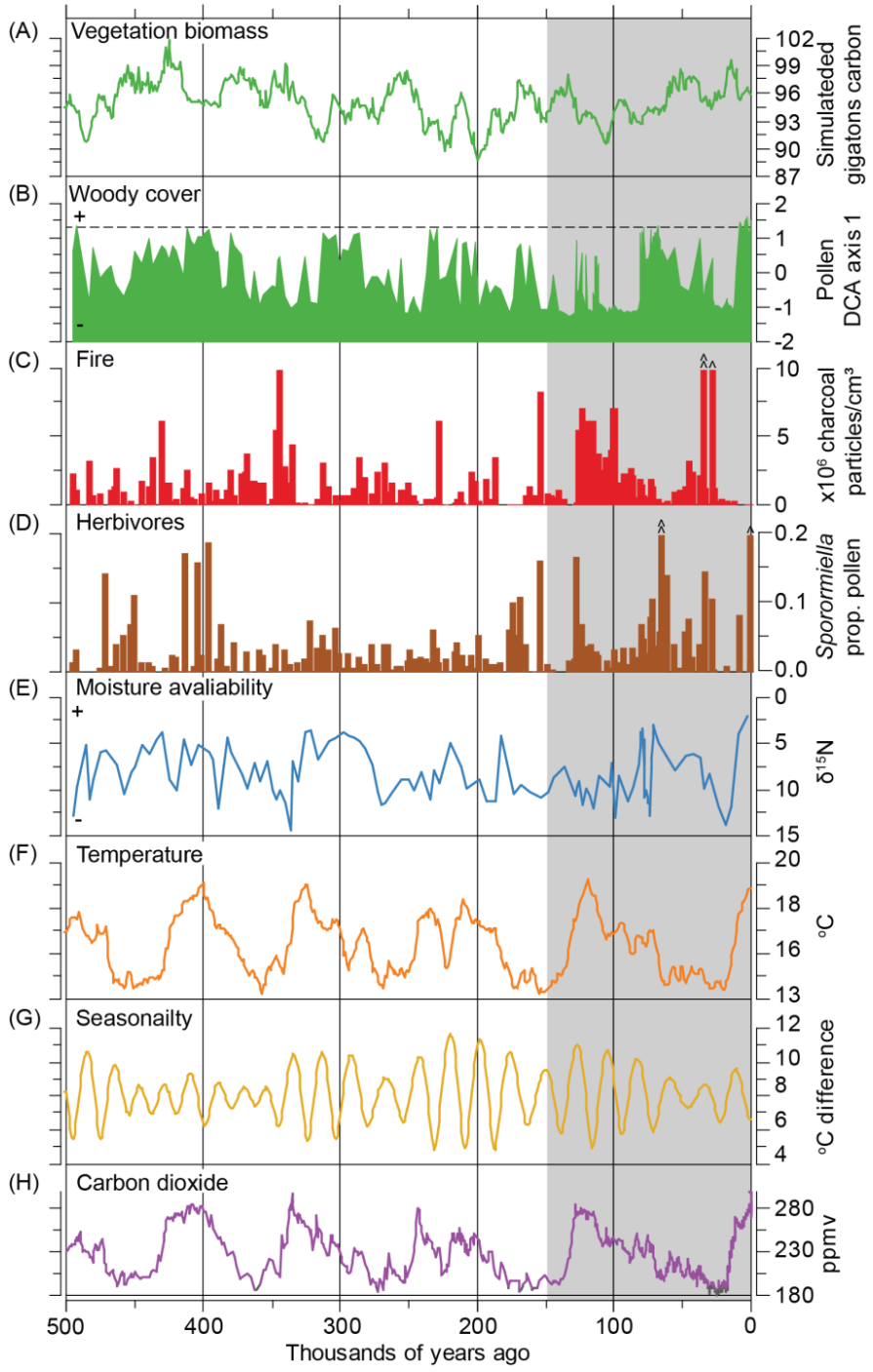

Fig. 1. Five hundred thousand years of tropical environmental change indicated by model simulations of conditions for low northern latitudes (0-23 ^{o}N) (panels A, F, G), empirical data from Lake Bosumtwi (Ghana) (panels B-E), and global atmospheric CO_2 (panel H). (A) Simulated vegetation carbon storage. (B) Characterization of the variation in the abundance of woody taxa within the overall pollen/spore assemblage data; + indicates more woody taxa, -

indicates higher abundance of grass (represented by the first ordination axis based on Detrended Correspondence Analysis: DCA axis 1). (C) Reconstructed fire activity from sedimentary charcoal abundance data; two values exceed the scales shown, sample indicated by ^^ = 25 and ^ = 16 x10^6 charcoal particles/cm^3. (D) Relative mammalian herbivore density reconstructed from sedimentary *Sporormiella* abundance; two samples exceed the scale shown, sample indicated by ^^ = 0.37 and ^ = 0.36 as a proportion of the pollen sum. (E) Moisture availability reconstructed from sedimentary $\delta^{15}N$; + indicates deeper lake levels, - indicates lower lake levels. (F) Simulated temperature for low northern latitude band. (G) Simulated difference in temperature between seasons for low northern latitude band, *i.e.,* high values indicate greater difference in temperature between seasons. (H) Atmospheric CO_2 (for further information see *(32)*). Grey box indicates data used within the *c.* 150,000-year time interval structural equation model (SEM) (Fig. 2B). The entire time range of the figure indicates the data used within the *c.* 500,000-year time interval SEM (Fig. 2C).

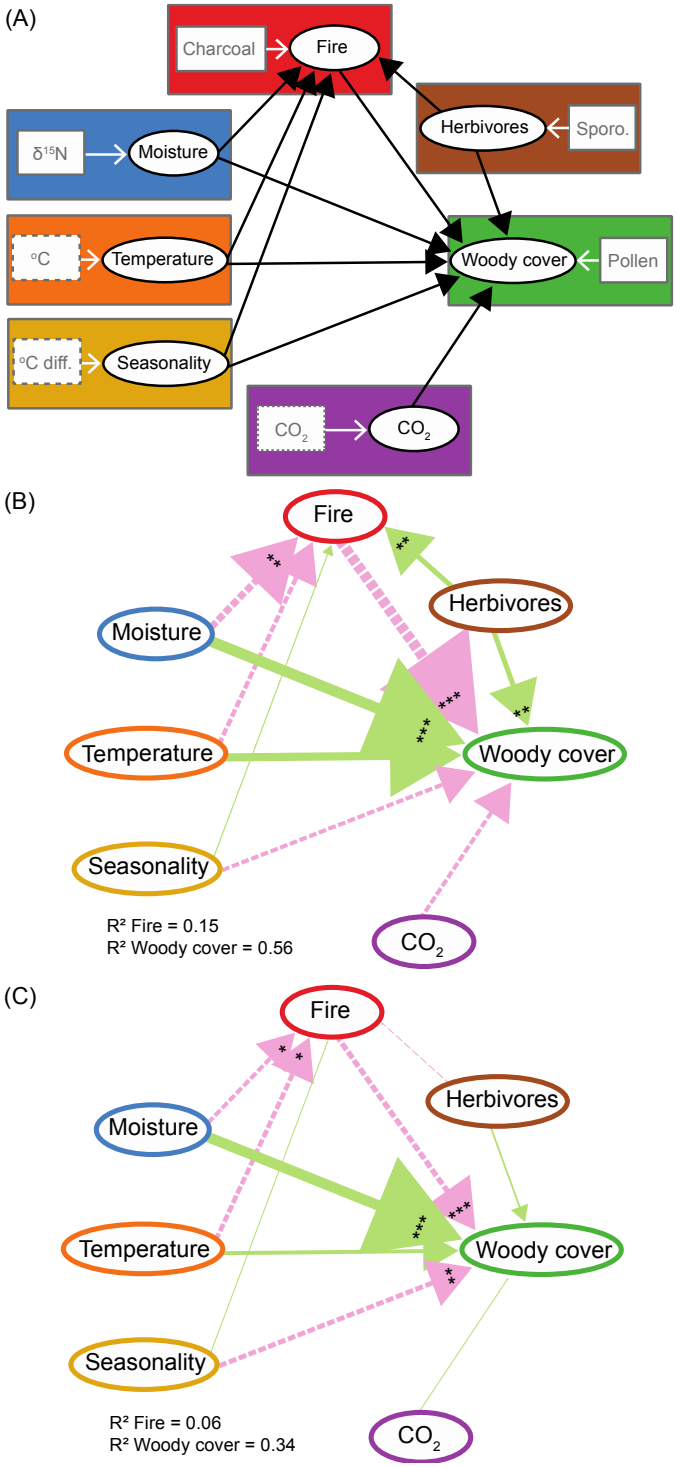

Fig. 2. Assessment of past relationships between climate, atmospheric CO_2, landscape processes, and vegetation in the tropics using a structural equation modeling approach. (A) Hypothesized relationships examined in this study (see Fig. 1). Results of structural equation modeling for (B) the last *c.* 150,000-years, and (C) the last *c.* 500,000-years based the weighted average chronology *(32)*. Measured variables are indicated by square gray boxes: solid lines indicate

empirical data derived from the Bosumtwi sedimentary record, dashes indicate data derived from the GENIE-1 model, and dots indicate empirical data from ice cores (see *(32)*). Latent variables are in black ovals. Colors associated with variables match Fig. 1. In panels (B) and (C) arrow color indicate positive (green, solid) and negative (pink, dashed) relationships, arrow thickness represents the absolute strength of the relationships based on the average age model *(32)*. Significance testing *: 0.01 <P <0.05, **: 0.001 <P <0.01, ***: <0.001. Full model results are presented in Table S1 *(32)*.

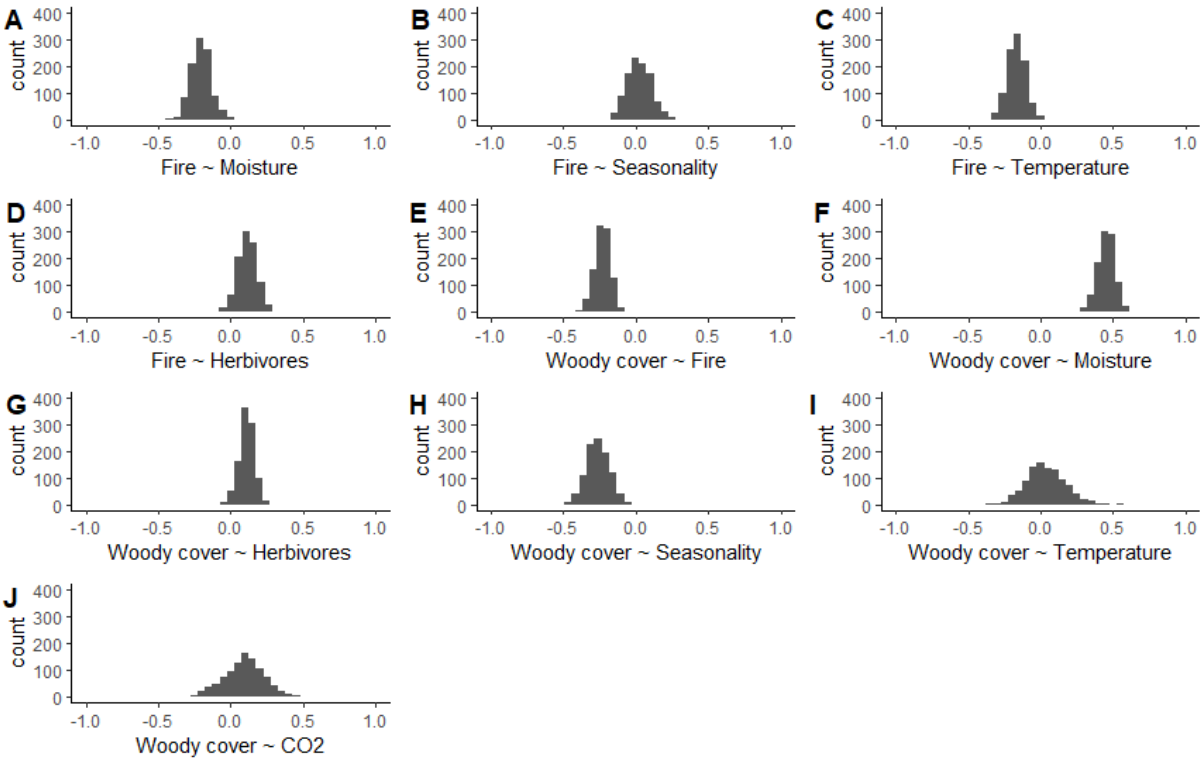

Fig. 3. Distributions of the standardized coefficients for the predictor variables in the structural equation models (SEMs) for the *c.* 500,000-year interval for Bosumtwi (Fig. 2C). The SEMs were run against 1000 possible alternative versions of the chronology to explore for possible bias due to chronological uncertainty. The predictor variables are shown per response variable (fire and woody cover). The most important drivers of woody cover are moisture availability and fire as they do not include zero in their distributions. The statistics are reported in *(32)*.

Science
AAAS

Supplementary Materials for

Long-term changes in moisture, not CO_2, are the primary driver of woody cover change in the tropics

William D. Gosling, Charlotte S. Miller, Timothy M. Shanahan, Philip B. Holden,
Jonathan T. Overpeck, and Frank van Langevelde
Correspondence to: W.D.Gosling@uva.nl

This PDF file includes:

Materials and Methods

Lake Bosumtwi chronology

An age model extending to the base of drill core 5B was constructed using a combination of radiocarbon (calibrated ^{14}C; n= 109), optically stimulated luminescence (OSL; n=22) and uranium-thorium (U/Th; n=5) dates *(53)*, as well as published dates for the age of the crater from the literature of 1.07 ± 0.05 million years *(54)*. The use of microtektite ages as a constraint on the base of the record is based on observations of impact related "accretionary" lapilli, microtektite-like glass spherules and shocked quartz in the basal sediments of core 5B at 290 meters below lake floor (mblf) *(55)*. Age-depth modeling was performed using a Bayesian approach in R software using the Bacon model *(56, 57)*.

The model used here is updated from that published in *(53)* and used previously in palynological studies of the long Bosumtwi record *(28, 29, 58, 59)*. First, we extended the age model to the base of the sediment record by including the crater age in the Bacon model, rather than by simple linear extrapolation *(29)*, which allows us to generate more robust age uncertainties for the deeper portion of the record. Second, we excluded the paleomagnetic excursions first presented in *(53)*. Additional work on the paleomagnetics in the sediments from Bosumtwi performed at the University of Rhode Island found that downcore identifications of paleomagnetic excursions in the record were unreliable (C. Heil, personal communication). As a result, we opted to remove them from the current age model until their identification can be confirmed. We also included all of the U-Th ages in the age model, given that even the large errors in the deepest sample (±85,000 years) result in it having a minimal impact on the resultant age model.

The Bacon age modeling approach has the advantage over more traditional age modeling approaches in that it provides an ensemble of possible age models given the age constraints, their analytical (and calibrated) age uncertainties and distributions, and sedimentation rates (grey shading, Fig. S1). Although any of these age models is possible, a weighted average chronology (solid line, Fig. S1) highlights the greater density of models towards the center of this distribution. In the current study, we use the weighted chronology in the structural equation models presented in Figure 2. To determine the potential influence of age model uncertainty on these results and the robustness of our conclusions, we also run our analysis on 1000 possible versions of the age models produced by Bacon *(60)*.

Lake Bosumtwi microfossil data

Two-hundred and seventeen sub-samples were extracted from the Lake Bosumtwi sediment core (BOS04-5B) and processed following standard palynological techniques, including treatment with hydroflouric acid and acetolysis *(61)*. Pollen and vegetation spore concentrations were calculated using the exotic marker *Lycopodium (62)*. Each sample was analyzed for pollen/spores, charcoal fragments and *Sporormiella* fungal spores, which are interpreted as indicators of vegetation change, fire activity, and mammalian herbivore density, respectively.

Pollen and spore assemblages have long been accepted as indicative of past vegetation cover *(63, 64)*, and the spatial extent of the vegetation cover represented by the pollen/spores within lake sediments is known to be proportional to the size of the lake *(65)*. Applying these principles to Bosumtwi, which was formed by a meteorite impact and is consequently circular in shape, approximately 10.5 km diameter with steep sided walls and a flat bottom *(55)*, it suggests that, although lake level fluctuations have occurred at Bosumtwi in the past *(29, 66)*, the

diameter of the lake is unlikely to have varied greatly. Therefore, the source area of the microfossils entering the lake is likely to have remained relatively constant through time and the pollen/spore signal can be confidently interpreted as indicative of genuine changes in the proportion of vegetation cover in the landscape around the lake. The source area of pollen/spores for a lake of *c.* 10 km diameter is estimated to be >90% "regional", i.e., from 100s meter distance from the lake *(65)*. The major variation in the vegetation change within the Bosumwti pollen/spore assemblage (characterized by the first axis of the Detrended Correspondance Analysis [DCA], see below) is driven by the abundance of grass (Poaceae) pollen *(29)*. For the majority of the last *c.* 500,000 years the abundance of Poaceae pollen is >40% indicative of open ecosystem (grassland savanna and wooded savanna) conditions similar to those found around 250 kms to the north of the lake today *(67)*. Therefore, although there are clear fluctuations in the proportion of woody cover throughout the last *c.* 500,000 years at Bosumtwi, we interpret the majority of the record before *c.* 9,000 years ago as indicative of vegetation cover more open than modern. In the last *c.* 9,000 years higher abundances of *Hymenocardia*, *Alchornea* and Arecaeae (including *Elaeis guineensis*/oil palm) make the assemblage distinct from any other seen in earlier periods in this record *(28)* likely related to human activity. Furthermore, we note that the new age vs. depth model presented here (see above) results in a shift in the timing of woody cover change inferred in previous publications *(29)* between 70,000 and 20,000 years ago; however, given the longer (*c.* 500,000 year) duration of the overall record we feel that this offset does not impact the main findings.

Microscopic remains were counted at x40 and x100 magnification on a Nikon Eclipse 50i microscope, identifications were based on published pollen atlases *(68-70)* and reference collection at The Open University (UK). The DCA was calculated based on the percentage data from all pollen/spore taxa reaching > 2% of the terrestrial pollen sum in at least one sample (total 43 taxa), with the first and main axis of variation found to relate closely to the degree of vegetation openness (abundance of Poaceae pollen); characteristic pollen taxa from savanna also include Amaranthaceae, Caryophyllaceae and *Securinega*, from deciduous woodland Combretaceae, *Mimosa*, and *Lannea*, and from tropical rainforest *Alchornea*, Arecaceae and *Macaranga*, Table S2 in *(29)*. Pollen/spore data, and the DCA to characterize the maximum variation within the data set, were previously presented *(28, 29)*; please see these publications for further details of the methodology.

Charcoal fragments are produced by fire activity and their abundance within lake sediments is widely regarded to reflect the amount of biomass burned *(71)*. Charcoal fragments are defined here as particles >10 μm that are present on slides following palynological preparation. Charcoal was identified following *(72)*. Counting of charcoal was done for each of the 217 sub-samples analyses for pollen/spores using the same slides; therefore these data sets are directly comparable. Concentrations of charcoal were calculated relative to the exotic marker *Lycopodium*. Charcoal concentrations from between *c.* 500,000 and 9,000 year ago were exceptionally high in nearly every sample (204 sub-samples with mean 1,705,563 fragments/cm^3, maximum 2,523,504 fragments/cm^3, minimum 1191 fragments/cm^3), while during the period 9,000 years ago to modern concentrations they were much lower (13 sub-samples with mean 22,621 fragments/cm^3, maximum 85,795 fragments/cm^3, minimum 0 fragments/cm^3). The vast majority of the charcoal fragments counted within the Bosumtwi sediments are interpreted as indicative of frequent burning of grass dominated, fire prone, vegetation around the lake because: (i) throughout most of the portion of the record where fire is

abundant Poaceae is the dominant pollen type *(28)*, and (ii) within the charcoal fragments grass stomata are preserved (Fig. S2). The charcoal data has not been previously published.

Sporormiella is a coprophilous fungus that grows on the dung of mammalian herbivores. The spores of *Sporormiella* preserved within lake sediments can be used to assess relative shifts in the density of mammalian herbivores within the landscape *(73, 74)*. *Sporormiella* was identified following *(75)*. Counting of *Sporormiella* was done in tandem with the pollen/spore counting; therefore these data sets are directly comparable. The abundance of *Sporormiella* was calculated as a proportion relative to the pollen sum, following *(76)*. In the Bosumtwi sediments *Sporormiella* spore abundance is near continually present from *c.* 500,000 until *c.* 22,000 years ago (194 sub-samples with mean 0.03, maximum 0.37, and minimum 0.00 proportion of the pollen sum), whereas from *c.* 22,000 until *c.* 800 years ago *Sporormiella* spores occur infrequently at low abundances (20 sub-samples with mean 0.01, maximum 0.08, and minimum 0.00 proportion of the pollen sum), while after *c.* 800 years ago *Sporormiella* abundance is highly variable (3 sub-samples in which proportions relative to the pollen sum were 0.00, 0.36, and 0.02); the high abundances during this period are likely due to the introduction of cattle to the area by people. *Sporormiella* spore abundances can vary in lake sediments dependent on the density of mammalian herbivores within the landscape and the proximity of the shore line *(77)*. Given the bathymetry of Bosumtwi the shore line is likely to have remained a relatively constant distance from the core site throughout the duration of sediment accumulation. Therefore, we interpret the changes in the abundance of *Sporormiella* spores within the sediments as broadly indicative of the relative density of mammalian herbivores within the surrounding landscape. The *Sporormiella* data has not been previously published.

The analytical uncertainty (95% confidence intervals) has been calculated for the entire pollen/spore data set *(29)*, and a portion of the record for charcoal and *Sporormiella (78).* These analyses indicate that the major trends in the data are robust and therefore that comparison of trends identified between the records is valid.

Nitrogen isotope data

One-hundred and twenty-three sub-samples were extracted from the Lake Bosumtwi sediment core (BOS04-5B) and analyzed for $\delta^{15}N$ following standard techniques *(79)*. The $\delta^{15}N$ is a proxy for moisture availability *(29, 66, 79)*. The full methods and $\delta^{15}N$ data were previously published *(29)*. In summary, sub-samples of around 0.6 g were extracted from the core and treated with 0.1 M HCl for 24 hours, then 1 M HCl for 24 hours, and finally rinsed to neutrality with Milli-Q water. Sub-samples were then dried, homogenized and the $\delta^{15}N$ determined using a Thermo Flash HT element analyzer. Data are expressed following *(80)*. The $\delta^{15}N$ values obtained from Bosumtwi have been interpreted to reflect changing lake level *(29)*. Lower values are interpreted to indicate higher lake levels because a deeper, more stratified lake, enhances the contribution of cyanobacteria ($\delta^{15}N$ value 0 ±2‰) relative to terrestrial plant (4.5-10.3‰) or aquatic plant (12.8‰) sources *(66)*. The $\delta^{15}N$ were previously published in *(29)*.

Temperature and seasonality data

Past temperature and seasonality data (seasonal difference in temperature) were extracted from a transient simulation of global climate performed with the GENIE-1 intermediate complexity Earth system (climate-carbon cycle) model *(35)*. GENIE-1 provides the computational efficiency required to perform: (i) long (multiple glacial cycle) simulations, and (ii) large ensembles of simulations to quantify model uncertainty. The physical model comprises a 3-D frictional

geostrophic ocean with eddy-induced and isopycnal mixing coupled to a 2-D fixed wind-field Energy-Moisture Balance Model (EMBM) atmosphere and a dynamic and thermodynamic sea-ice component *(81)*. These are coupled to a minimum spatial model of vegetation carbon, soil carbon and soil water storage *(82)*. The model setup and boundary conditions are described in detail in *(35)*. In summary, changing atmospheric CO_2 is prescribed from ice core records *(83)*, while other greenhouse gases are neglected. Orbital forcing is from Berger (1978) *(84)*. Transient Laurentide and Eurasian Ice Sheets are represented by interpolating the spatial distribution of Ice-4G *(85)* onto the benthic $\delta^{18}O$ record *(86)*. Outputs from the simulation were sub-divided into five latitudinal bands *(33)*, of which the data from the low northern latitudinal band (0-23^{o}N) are used here.

The temporal variability within the model is based upon the high-quality chronologies established for the ice core CO_2 record *(83)*, benthic $\delta^{18}O$ *(86)*, and orbital forcing *(84)*. The temporal variability of the simulation outputs have been previously validated against Antarctic surface temperature and Atlantic sea surface temperature *(35)*. We here use an existing ensemble of simulations over the last glacial cycle *(33)* to explore simulated temporal uncertainties. The ensemble uses an identical model setup and forcing to our base case analysis but applies 174 parameter sets which are a subset of the 480-member 'Last Glacial Maximum plausibility-constrained' parameter set *(87)*. These parameter sets all exhibit plausible pre-industrial and Last Glacial Maximum climates and vegetation states, filtered by the additional constraint that they exhibit a collapse of Atlantic Meridional Overturning during glacial terminations *(35)*. We extract the ensemble time series of warming over latitude band 0 to 23°N, which we plot in Fig S3: (a) in absolute terms, and (b) standardised to a mean of 0 and a standard deviation of 1 as appropriate for our structural equation modelling. The signal is highly robust with respect to modelling uncertainties, with individual simulations exhibiting a mean R^2 of 99% with respect to the ensemble mean.

Atmospheric CO_2 data

Past atmospheric CO_2 data were derived from published Antarctic ice core records *(83)*, and were embedded within the GENIE-1 model as a transient boundary condition *(35)*.

Structural equation modelling

Structural equation modelling (SEM) is used to understand causal relationships in systems by evaluating the statistical fit between expectation based on theory and empirical data. We choose SEM because it has proven insightful for testing hypotheses of causal interactions in ecological systems *(88)*, and because we sought to evaluate direct and indirect relationships among variables which could translate into general theory relating to the drivers of tropical vegetation. The focus on causal relationships by analysing direct and indirect relationships is one aspect that sets SEM apart from other multivariate methods. For example, SEM provides a way to evaluate the direct effect of fires on vegetation after controlling for the joint effects of environmental drivers on fire and vegetation.

At the core of our SEM analysis is an *a priori* conceptual model which describes, schematically, how our six drivers may interact to determine vegetation (Fig. 2A; Table S1). Arrows in the diagram represent direct causal influences of one variable on another, including specifying the directionality (i.e., positive or negative), but not the shape (e.g., degree of linearity) of the relationship. The conceptual model is based on our current understanding of determinants for tropical vegetation (e.g. *(25-27, 31)*). As SEM allows both the direct and

indirect effects of predictor variables to be tested, we included in our model the direct and indirect of effect of rainfall on woody cover (following the discussion, see e.g. *(27)*) by using fire as response variable. We fitted the measured variables to the SEM. While we acknowledge the potential for non-linear effects in vegetation (e.g., *(89)*) our approach was to seek a simple, multivariate model based on linear relationships, to assess the relative importance of drivers.

Prior to running the SEM three data transformations were performed. First, we multiplied the $\delta^{15}N$ data with -1 as low values for $\delta^{15}N$ represent high moisture availability. After multiplication, low values mean low moisture values. Second, we transformed *Sporormiella* to the power 0.3 and charcoal to the power 0.2 to reduce the effect of a few samples with large values and to approximate a normal distribution. Third, we scaled all the predictors to a mean of 0 and standard deviation of 1. The next step in the modelling process was to create a SEM which included all possible effects of the predictors on fire occurrence and woody cover plus the direct effect of fire occurrence on woody cover. We used the 'sem' function from the R package 'lavaan' *(90)*. The final model was estimated with the MLM procedures computing a Satorra-Bentler scaled (mean adjusted) test to obtain χ^2 values based on expected versus observed covariance matrices, which are standard goodness-of-fit measures in SEM. The Satorra–Bentler scaled χ^2 test is robust to nonnormality (especially for the variable woody cover). The resulting path coefficients from a predictor to a response variable depict the standardized relative effect on the response variable.

Besides the hypothesized direct and indirect relationships (Fig. 2A), we also added correlations between the measured variables: temperature ~~ CO_2, temperature ~~ seasonality, temperature ~~ moisture, and fire ~~ CO_2. The correlational relationships between the variables are given in Table S1. In Figure S5, Spearman rank correlations are given for all pairs of variables in our SEM for the data set of *c.* 500,000 years. The correlation between temperature and CO_2 is very strong as it is prescribed a boundary condition within the GENIE model set up (see above and *(35)*). Therefore, we did not test the effect of CO_2 on temperature, but corrected for its strong correlation in the SEM.

For the data set of *c.* 150,000 years, the SEM from Fig. 2B converged successfully after 40 iterations, and the data showed a very close fit to the model according to goodness of fit statistics (robust model: $\chi^2 = 5.885$, df = 7, P = 0.553, n = 114). The relationships of the model are depicted in Figure S4. For the data set of *c.* 500,000 years, the data also converged successfully to the same model from Fig. 2C after 35 iterations (robust model: $\chi^2 = 4.161$, df = 7, P = 0.761, n = 214). The distributions of the parameter estimates of the 1000 iterations for the data set of *c.* 500,000 years are presented in Fig. 3. For the 1000 iterations based on the data set of *c.* 150,000 years, the distribution of the parameter estimates are given in Fig. S6. Both sets of distributions show similar patterns with the most important variables moisture availability and fire not including zero in their distributions of the parameter estimates. We further explored our results by testing different models using SEM. First, we excluded temperature (and also the correlation between temperature ~~ CO_2) to test whether the presence of temperature would biasing the effect of CO_2. However, we could not fit the model to the data (for the *c.* 500,000-years dataset, $\chi^2 = 440.911$, df = 9, P < 0.001, n = 214). Excluding CO_2 gave us a model that fitted the data ($\chi^2 = 1.263$, df = 4, P = 0.868, n = 214) with a significant positive effect of temperature on woody cover (standardized parameter estimate = 0.166 ± 0.054 SE, P = 0.002). Running the model with only CO_2, temperature and/or temperature seasonality also did not result in models that fitted the data (P < 0.05). Finally, we tested the relationships between the drivers and woody cover using multiple regression, which allowed us to check whether temporal autocorrelation could have an

effect on the outcomes. Multiple regressions based on the *c.* 500,000-year dataset were done using either temperature or CO_2, given the high VIF values when combining them in the same model. We only found a significant relationship between CO_2 and woody cover in the presence of moisture availability and absence of temperature, but the standardised parameter estimate for CO_2 (0.153) was smaller than the one for moisture availability (0.414) using the *c.* 500,000 years dataset, similar results that we found with the SEM. The comparison between the linear regression model (using 'lm' in R) and the generalized least squares regression (using 'gls' in the R-package 'nlme') with first order auto-regressive (AR1) structure showed that the first had a better fit than the latter (based the AIC using 'model.sel' of the R-package 'MuMIn'). We concluded that temporal autocorrelation was not biasing our analyses. The results were qualitatively similar for the *c*. 150,000-years dataset.

CO_2 and other records of past vegetation change from Africa

In addition to Bosumtwi four records of past vegetation change exist from terrestrial locations in Africa that provide multi-millennial timeseries of past vegetation change on the glacial-interglacial (>100,000 year) timescales over which high magnitude (*c.* 100 ppm) fluctuations in atmospheric CO_2 are known to occur *(83)*. The longest records come from the eastern African rift valley: (i) Lake Magadi (drill core HSPDP-MAG14-2A; 1° 51' S, 36° 16' E) yielded a *c.* 992,000 year record, and is today surrounded by semi-desert grassland and shrubland, with *Acacia-Commiphora* deciduous bush at higher elevations vegetation *(40, 41)*, and (ii) Lake Malawi (drill cores MAL05-1B and MAL05-1C; 11° 18' S, 34° 26' E) yielded a *c.* 636,000 year record, and is today surrounded predominantly by miombo woodland, with Afromontane forest at higher elevation and tropical seasonal forest along some waterways *(42)*. Two shorter records that cover a significant portion of the last glacial-interglacial cycle come from Vankervelsvlei in southern Africa (drill core VVV10.1; 34° 0.7' S, 22° 54.2' E) which is today surrounded by Fynbos vegetation *(44, 91)*, and Lake Bambili in central Africa (6° 0' 19.56" N, 10° 15' 46.14" E) which is today surrounded by montane forest *(45, 92)*. If global CO_2 were driving woody cover change across Africa we would anticipate a uniform trend in increasing woody cover (decreasing abundance of grass) across these sites to be evident, and for these trends to be coincident with variation in global atmospheric CO_2. To gain a first order approximation of these relationships we have replotted previously published, and openly available, pollen (vegetation) data from the four sites (Fig. S7) that is used as proxy for grass abundance, and compare them to each other, Bosumtwi and global atmospheric CO_2 through a correlation analysis (Fig. S8); for the correlation analysis all records were resampled relative to the CO_2 record. Our analysis reveals no consistent trend between the different sites, or with atmospheric CO_2. The absence of any consistent pattern suggests that regionally specific factors, such as precipitation patterns, fire regimes or herbivore densities, are likely of greater importance to determining vegetation at these sites over long timescales than the fertilisation effect of atmospheric CO_2.

Figures

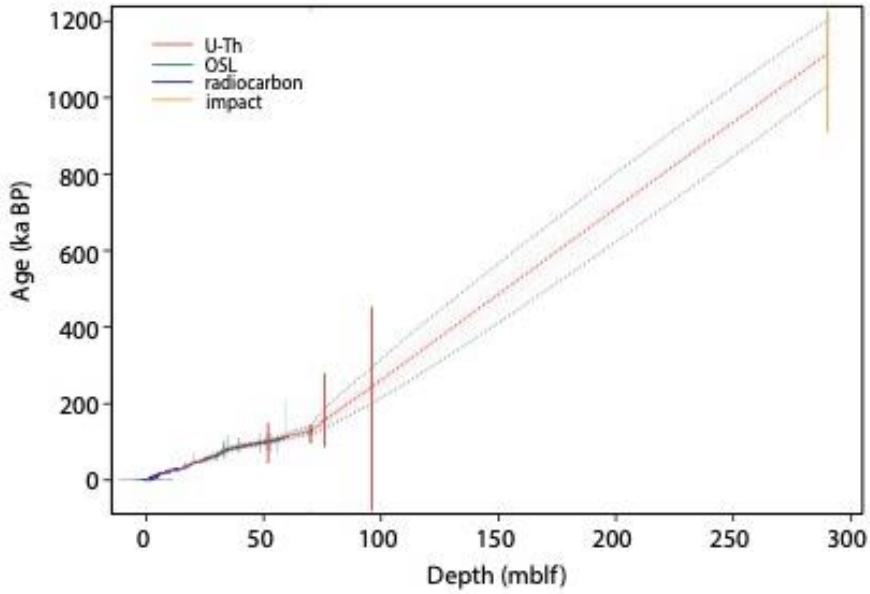

Fig. S1. Age-depth model generated by Bacon for Lake Bosumtwi. Lines show 2x standard deviation uncertainty ranges for radiocarbon (blue), optically stimulated luminescnce (green), uranium-thorium (red) and the impact (orange) age. Dashed red line is the weighted mean age, the grey shading indicates the density of Bacon-derived age models. Depths are in meters below lake floor (mblf) on the standardized age model for core 5B *(53)*.

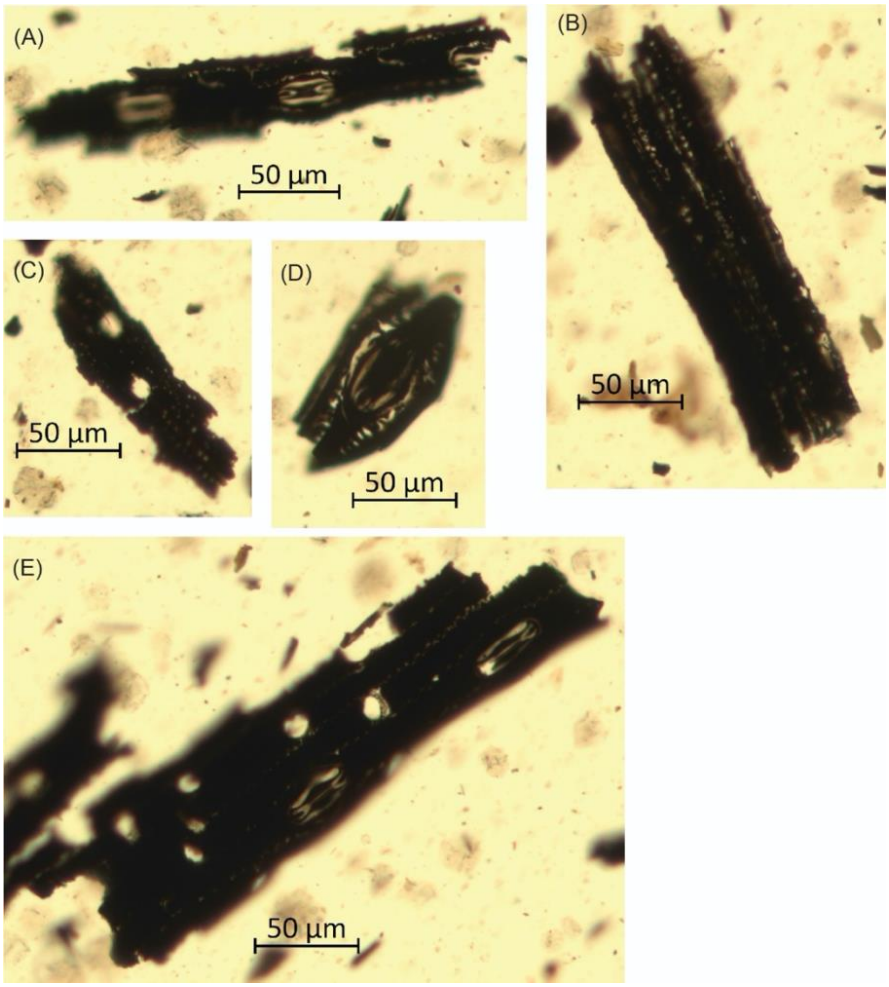

Fig. S2. Examples of grass micro-charcoal fragments from Lake Bosumtwi (sub-sample 21H1-45cm). Identification based on comparison with images contained in *(93)*.

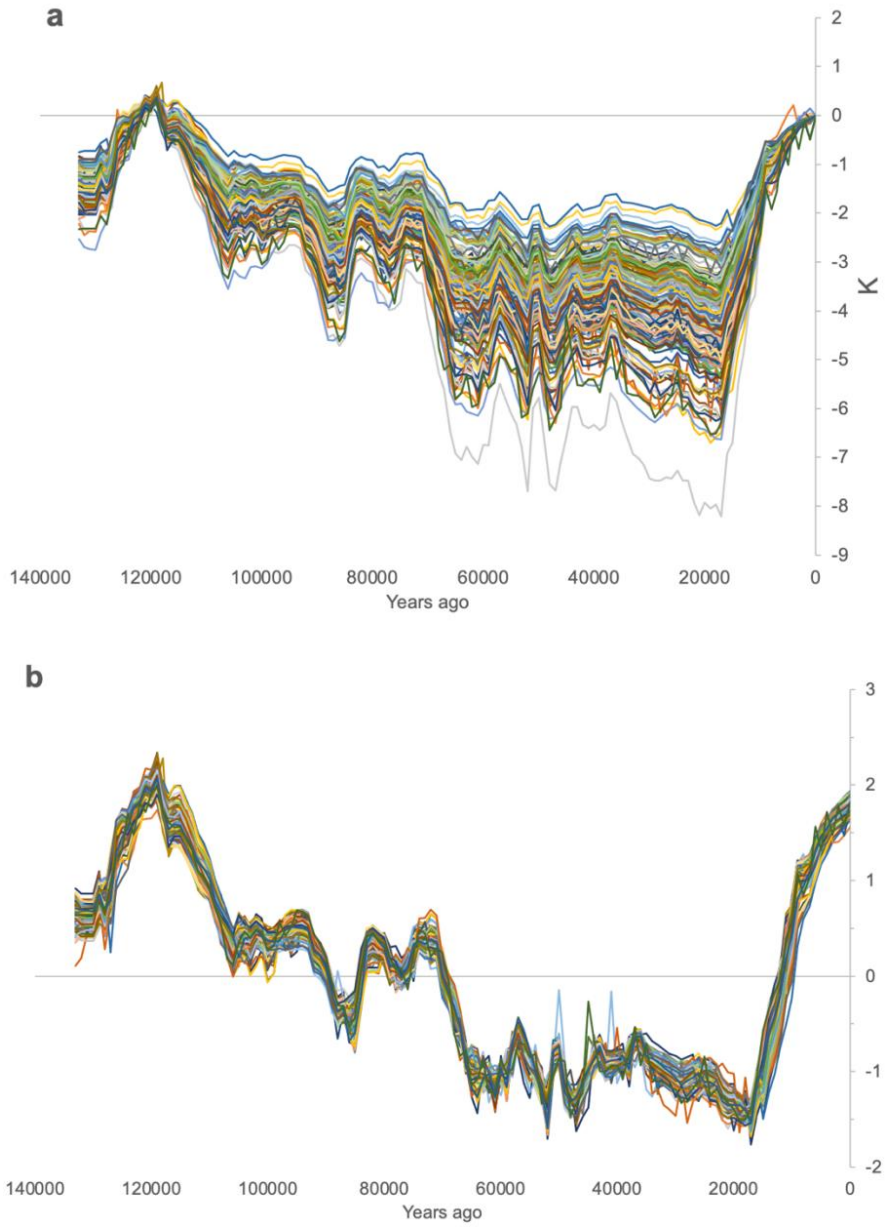

Fig. S3. Surface air temperature anomaly of an ensemble of simulations over the last glacial cycle performed in the GENIE-1 model *(33)*. Data are averaged over latitude band 0 to 23°N: (a) absolute anomalies, and (b) standardised anomalies with regard to preindustrial conditions.

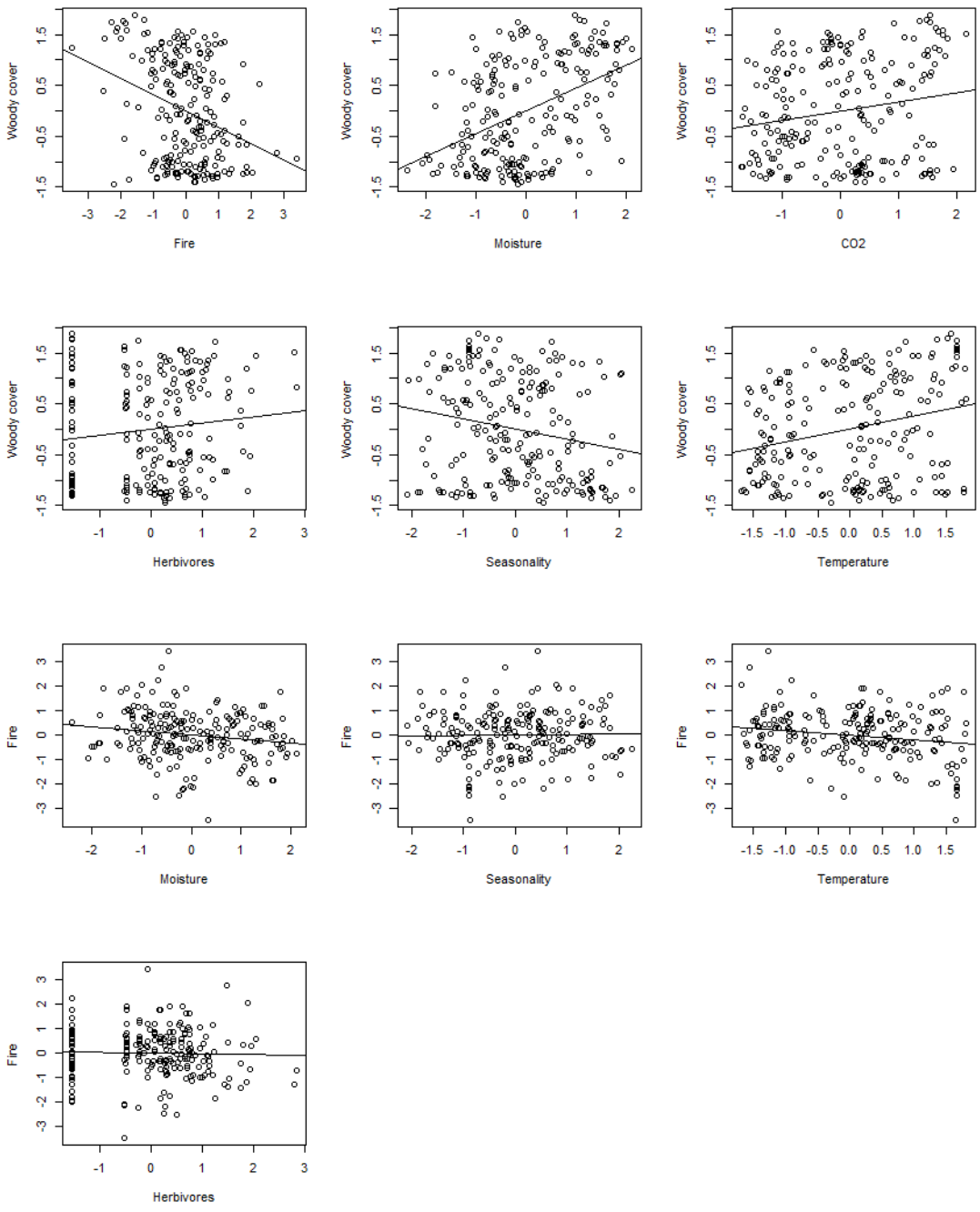

Fig. S4. The tested relationships of the scaled variables in the structural equation model based on the *c.* 500,000-year data set (shown in Fig. 2C and Table S1, along with parameter estimates and statistical significance).

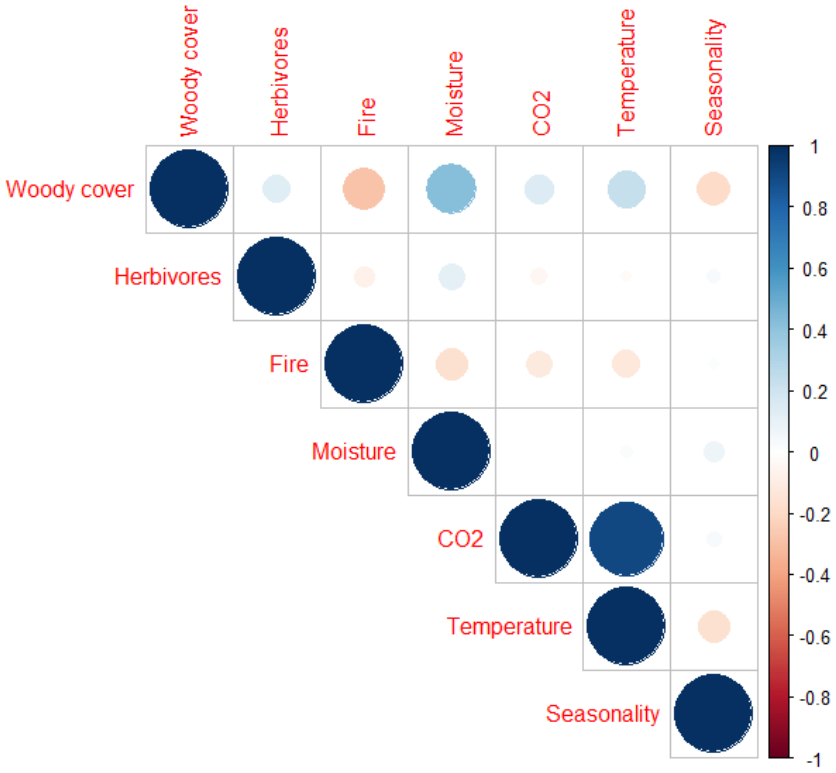

Fig. S5. Spearman rank correlations between the measured variables in the structural equation model based on the *c.* 500,000-year data set (Fig. 2C).

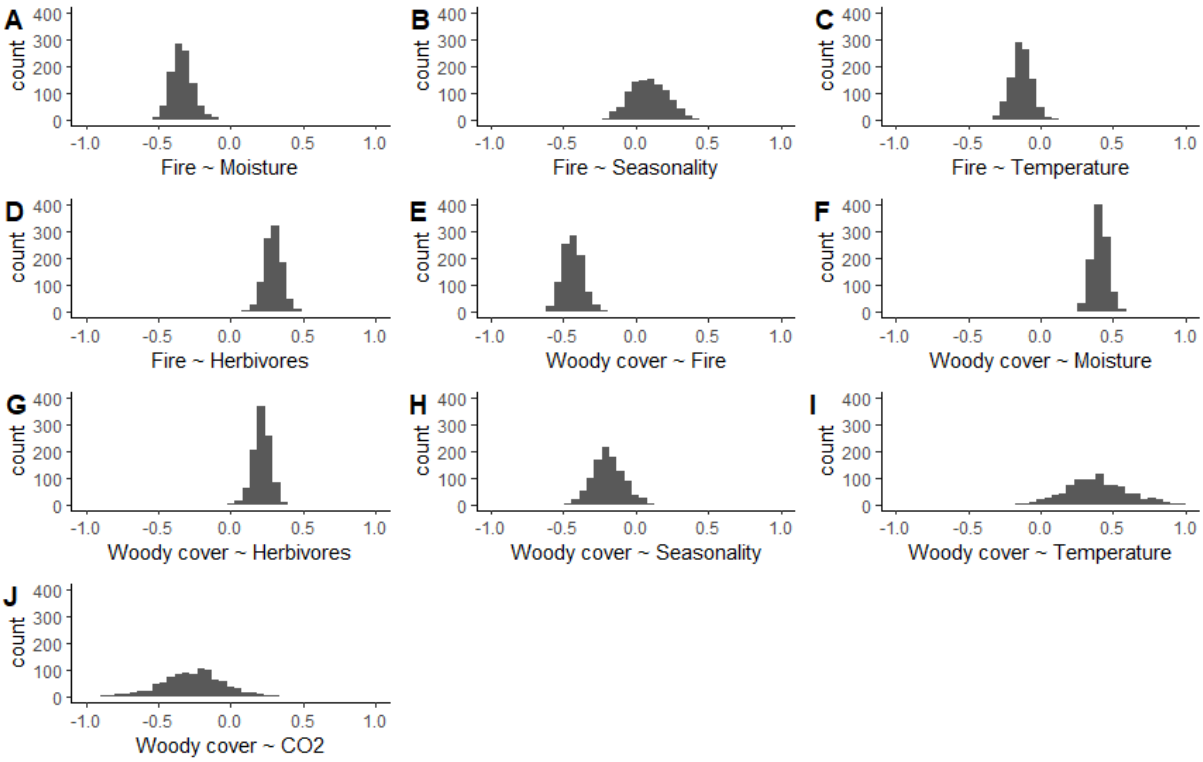

Fig. S6. Distributions of the standardized estimates for the predictor variables in the structural equation models (SEMs) for the *c.* 150,000-year interval for Bosumtwi (Fig. 2B). The SEMs were run against 1000 possible alternative versions of the chronology to explore for possible bias due to chronological uncertainty. The predictor variables are shown per response variable (fire and woody cover). The most important drivers of woody cover are moisture availability and fire. The statistics are reported in Table S1.

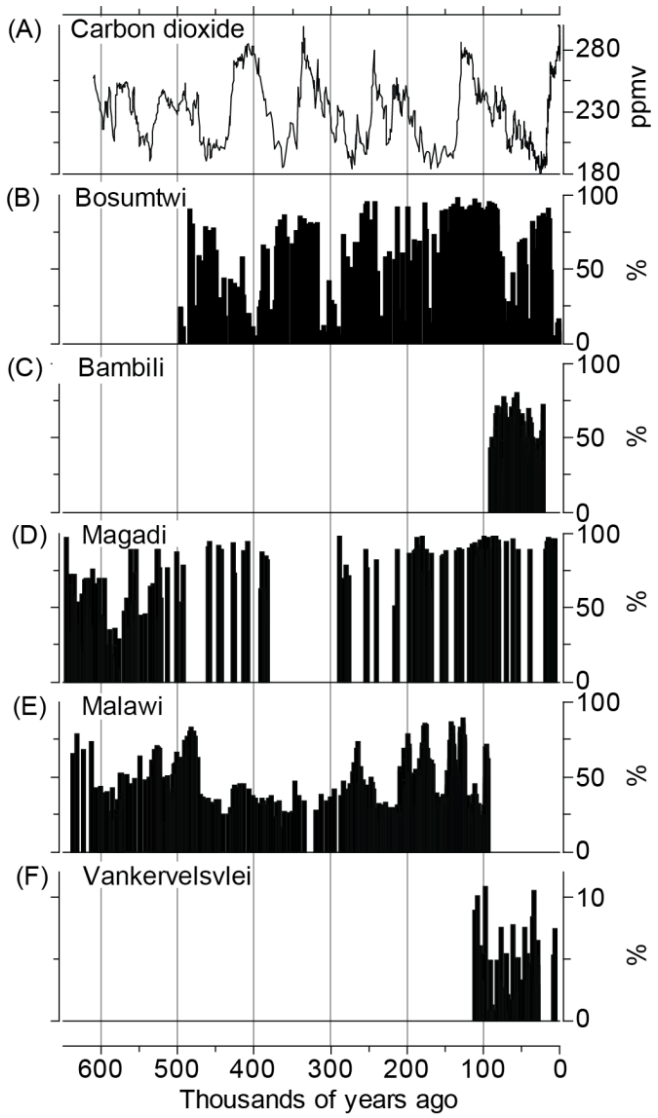

Fig. S7. Vegetation change from terrestrial records across Africa relative to global CO_2 change. (A) Carbon dioxide *(83)*. Percentage abundance of Poaceae (grass) pollen relative to the total pollen sums (organized latitudinally north to south) from: (B) Lake Bosumtwi *(60)*, (C) Lake Bambili *(45, 92)*, (D) Lake Magadi *(40)*, (E) Lake Malawi *(42)*, and (F) Vankervelsvlei *(44, 91)*.

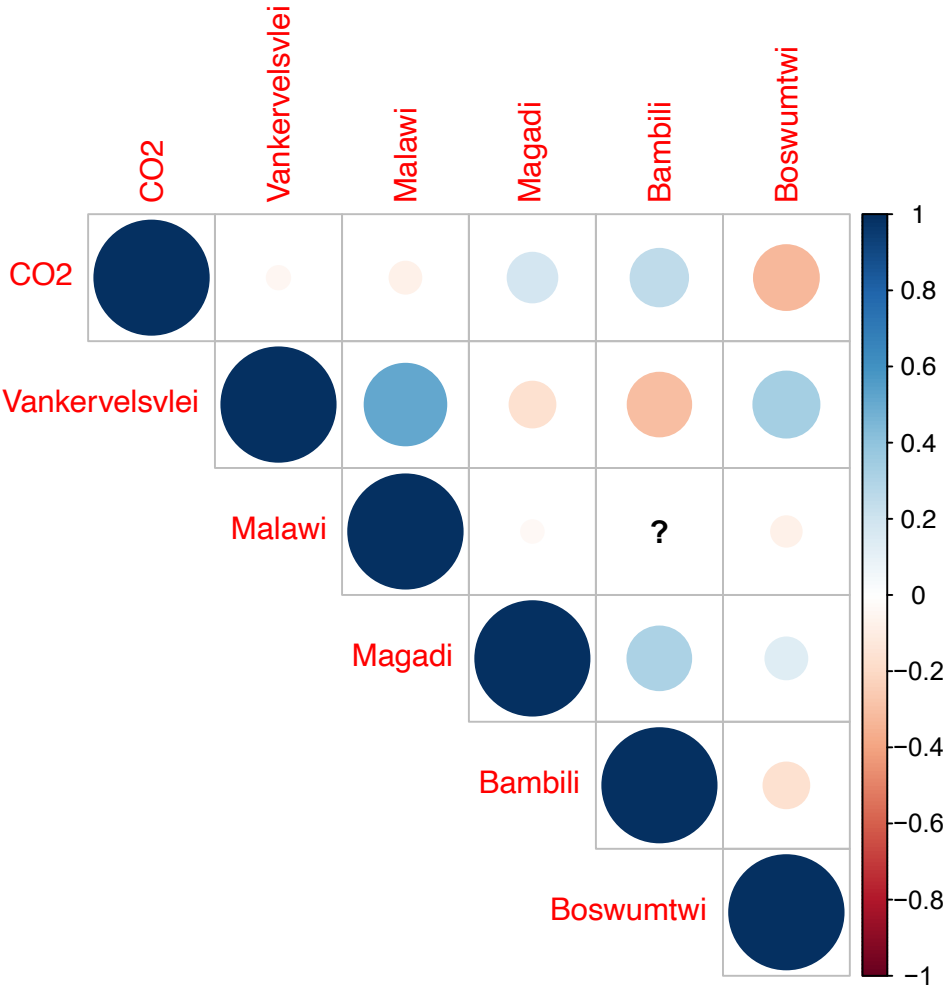

Fig. S8. Spearman rank correlations between pollen (vegetation) data from five sites (used as proxy for grass abundance, Fig. S7) and atmospheric CO_2. The question mark indicates that there is no overlap in data from the two sites Malawi and Bambili.

Table S1.

Results from the structural equation models based on the *c.* 150,000 years and *c.* 500,000 years data. For every model, the standardised parameter estimates (Est), standard error of the estimate (SE) and P-value of the predictors, and the correlational relationships between the predictor variables (~~) are given. Also the sample size N, the degrees of freedom df, the test statistic χ^2, the P-value of the model and the R^2 of the response variables are given.

	c. 150,000 years data			*c.* 500,000 years data		
	Est	SE	P	Est	SE	P
Fire ~						
Moisture	-0.274	0.080	0.001	-0.159	0.063	0.012
Seasonality	0.046	0.084	0.580	0.008	0.063	0.898
Temperature	-0.178	0.097	0.068	-0.182	0.076	0.016
Herbivores	0.200	0.074	0.007	-0.010	0.067	0.877
Woody cover ~						
Fire	-0.419	0.075	<0.001	-0.216	0.056	<0.001
Moisture	0.423	0.061	<0.001	0.406	0.054	<0.001
Herbivores	0.196	0.058	0.001	0.071	0.052	0.177
Seasonality	-0.159	0.089	0.074	-0.192	0.071	0.006
Temperature	0.319	0.241	0.185	0.157	0.141	0.265
CO_2	-0.163	0.242	0.500	0.010	0.137	0.942
Temperature ~~ CO_2	0.948	0.083	<0.001	0.912	0.059	<0.001
Temperature ~~ Seasonality	-0.173	0.028	<0.001	-0.196	0.030	<0.001
Temperature ~~ Moisture	0.057	0.023	0.015	0.053	0.027	0.053
Fire ~~ CO_2	-0.066	0.019	0.001	-0.019	0.025	0.453
N	114			214		
df	7			7		
χ^2	5.885			4.161		
P-value	0.553			0.761		
R^2 Fire	0.152			0.063		
R^2 Woody cover	0.564			0.344		

Supplementary References

53. T. M. Shanahan *et al.*, Age models for long lacustrine sediment records using multiple dating approaches - An example from Lake Bosumtwi, Ghana. *Quaternary Geochronology.* **15**, 47-60 (2013).
54. C. Koeberl, W. Reimold, J. Blum, C. P. Chamberlain, Petrology and geochemistry of target rocks from the Bosumtwi impact structure, Ghana, and comparison with Ivory Coast tektites. *Geochimica et Cosmochimica Acta.* **62**, 2179-2196 (1998).
55. C. Koeberl *et al.*, An international and multidisciplinary drilling project into a young complex impact structure: The 2004 ICDP Bosumtwi Crater Drilling Project - An overview. *Meteoritics and Planetary Science.* **42**, 483-511 (2007).
56. M. Blaauw, J. A. Christen, Flexible paleoclimate age-depth models using an autoregressive gamma process. *Bayesian Analysis.* **6**, 457-474 (2011).
57. M. Blaauw, Methods and code for 'classical' age-modelling of radiocarbon sequences. *Quaternary Geochronology.* **5**, 512-518 (2010).
58. P. E. Jardine *et al.*, Pollen and spores as biological recorders of past ultraviolet irradiance. *Scientific Reports.* **6**, 39269 (2016).
59. P. E. Jardine *et al.*, Sporopollenin chemistry and its durability in the geological record: an integration of extant and fossil chemical data across the seed plants. *Palaeontology.* **64**, 285-305 (2021).
60. W. D. Gosling *et al.*, Data from: Long-term changes in moisture, not CO2, are the primary driver of woody cover change in the tropics. *FigShare.* (2022). DOI: 10.6084/m9.figshare.18319466
61. P. D. Moore, J. A. Webb, M. E. Collinson, *Pollen Analysis* (Blackwell Scientific, Oxford, ed. 2nd, 1991).
62. J. Stockmarr, Tablets with spores used in absolute pollen analysis. *Pollen et Spore.* **XIII**, 615-621 (1971).
63. L. von Post, Forest tree pollen in south Swedish peat bog deposits. *Pollen et Spore.* **9**, 375-401 (English translation by M.B. Davis and K. Faegri from original 1916 lecture; Introduction by K. Faegri and J. Iversen) (1967).
64. H. Godwin, *The History of the British Flora: A Factual Basis for Phytogeography* (Cambridge University Press, Cambridge, 1956).
65. J. G. L. Jacobson, R. H. W. Bradshaw, The selection of sites for paleovegetational studies. *Quaternary Research.* **16**, 80-96 (1981).
66. M. R. Talbot, T. Johannessen, A high resolution palaeoclimatic record for the last 27 500 years in tropical West Africa from the carbon and nitrogen isotopic composition of lacustrine organic matter. *Earth & Planetary Science Letters.* **110**, 23-37 (1992).
67. A. C. M. Julier *et al.*, The modern pollen-vegetation relationships of a tropical forest-savannah mosaic landscape, Ghana, West Africa. *Palynology.* **42**, 324-338 (2018).
68. W. D. Gosling, C. S. Miller, D. A. Livingstone, Atlas of the tropical West African pollen flora. *Review of Palaeobotany and Palynology.* **199**, 1-135 (2013).
69. R. Bonnefille, Atlas des pollens d'Ethiopie. *Adansonia.* **11**, 463-518 (1971).
70. R. Bonnefille, G. Riollet, *Pollens des Savanes d'Afrique Orientale* (CNRS, Paris, 1980), pp. 140.
71. J. R. Marlon *et al.*, Global biomass burning: A synthesis and review of Holocene paleofire records and their controls. *Quaternary Science Reviews.* **65**, 5-25 (2013).

72. C. Whitlock, C. Larsen, in Tracking Environmental Change Using Lake Sediments Volume 3: Terrestrial, Algal and Siliceous Indicators, J. P. Smol, H. J. B. Birks, W. M. Last, Eds. (Kluwer Academic Publishers, Dordrecht/Boston/London, 2001), pp. 75-98.
73. O. K. Davis, D. S. Shafer, Sporormiella fungal spores, a palynological means of detecting herbivore density. *Palaeogeogr., Palaeoclimatol., Palaeoecol.* **237**, 40-50 (2006).
74. A. G. Baker, P. Cornelissen, S. A. Bhagwat, F. W. M. Vera, K. J. Willis, Quantification of population sizes of large herbivores and their long-term functional role in ecosystems using dung fungal spores. *Methods in Ecology and Evolution.* **7**, 1273-1281 (2016).
75. B. van Geel, A. Aptroot, Fossil ascomycetes in Quaternary deposits. *Nova Hedwigia.* **82**, 313-329 (2006).
76. J. L. Gill, J. W. Williams, S. T. Jackson, K. B. Lininger, G. S. Robinson, Pleistocene megafaunal collapse, novel plant communities, and enhanced fire regimes in North America. *Science.* **326**, 1100-1103 (2009).
77. D. Raper, M. Bush, A test of Sporormiella representation as a predictor of megaherbivore presence and abundance. *Quaternary Research.* **71**, 490-496 (2009).
78. W. D. Gosling *et al.*, Preliminary evidence for green, brown and black worlds in tropical western Africa during the Middle and Late Pleistocene. *Palaeoecology of Africa.* **35**, 13-25 (2021).
79. M. R. Talbot, in Tracking Environmental Change Using Lake Sediments. Volume 2. Physical and Geochemical methods, W. M. Last, J. P. Smol, Eds. (Kluwer Academic Press, Dordrecht/Boston/London, 2001), pp. 401-439.
80. T. B. Coplen, Guidelines and recommended terms for expression of stable-isotope-ratio and gas-ratio measurement results. *Rapid Communications in Mass Spectrometry.* **25**, 2538-2560 (2011).
81. N. R. Edwards, R. Marsh, Uncertainties due to transport-parameter sensitivity in an efficient 3-D ocean-climate model. *Clim. Dyn.* **24**, 415-433 (2005).
82. M. S. Williamson, T. M. Lenton, J. G. Shepherd, N. R. Edwards, An efficient numerical terrestrial scheme (ENTS) for Earth system modelling. *Ecological Modelling.* **198**, 362-374 (2006).
83. D. Lüthi *et al.*, High-resolution carbon dioxide concentration record 650,000–800,000 years before present. *Nature.* **453**, 379-382 (2008).
84. A. Berger, Long-term variations of daily insolation and Quaternary climatic change. *Journal of Atmospheric Science.* **35**, 2362-2367 (1978).
85. W. R. Peltier, Ice age paleotopography. *Science.* **265**, 195-201 (1994).
86. L. E. Lisiecki, M. E. Raymo, A Pliocene-Pleistocene stack of 57 globally distributed benthic d18O records. *Paleoceanography.* **20**, PA1003 (2005).
87. P. B. Holden, N. R. Edwards, K. I. C. Oliver, T. M. Lenton, R. D. Wilkinson, A probabilistic calibration of climate sensitivity and terrestrial carbon change in GENIE-1. *Clim. Dyn.* **35**, 785-806 (2010).
88. B. H. Pugesek, A. Tomer, A. von Eye, Eds., *Structural Equation Modelling: Applications in Ecological and Evolutionary Biology* (Cambridge University Press, Cambridge, 2003).
89. M. Austin, On non-linear species response models in ordination. *Vegetatio.* **33**, 33-41 (1976).
90. Y. Rosseel, lavaan: An R Package for Structural Equation Modeling. *Journal of Statistical Software.* **48**(2012).
91. L. J. Quick *et al.*, Neotoma Dataset 46707: Vankervelsvlei. (2016).
92. A.-M. Lézine, L. Février, K. Lemonnier, Neotoma Dataset 40945: Bambili 2. (2019).

93. P. G. Palmer, S. Gerbeth-Jones, A scanning electron microscope survey of the epidermis of East African grasses, V, and West African supplement. *Smithsonian Contributions to Botany*. **67**, 1-157 (1988).